

Cycloaddition Reactions of Metalloaromatic Complexes of Iridium and Rhodium: A Mechanistic DFT Investigation

Mark A. Iron, Jan M. L. Martin,* and Milko E. van der Boom*

Contribution from the Department of Organic Chemistry, Weizmann Institute of Science, 76100 Rehovot, Israel

Received June 17, 2003; E-mail: comartin@wicc.weizmann.ac.il; milko.vanderboom@weizmann.ac.il

Abstract: The mechanistic details of 1,2- and 1,4-cycloaddition reactions of acetone, CO₂, and CS₂ to isostructural iridiabenzene, iridiapyrylium, and iridiathiabenzene complexes, as well as their rhodium analogues, were elucidated by density functional theory (DFT) at the PCM/mPW1K/SDB-cc-pVDZ//mPW1K/SDD level of theory. The calculated reaction profiles concur with reported experimental observations. It was found that the first complex reacts via a concerted reaction mechanism, while the latter two react by a stepwise mechanism. Several factors affecting the reaction mechanisms and outcome were identified. They include the composition and size of the metal-aromatic ring, the length of the substrate C=X (X = O, S) bond, the geometry of the product, the symmetry of the frontier molecular orbitals, and the type of reaction mechanism involved.

Introduction

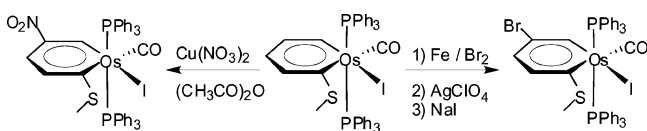
Kekulé's discovery of the aromatic nature of benzene was possibly one of the greatest landmarks in chemistry.¹ The impact has been felt in most fields of science. Aromaticity plays an important role in organic, industrial, and medicinal chemistry, and in life sciences where four amino acids (phenylalanine, tyrosine, tryptophan, and histidine) contain aromatic rings. Subsequent research included substituting one or more CH units of benzene. Initially this involved elements such as N, O, P, and S, but later progress included main group metals (e.g., B,² Si,^{3,4} Ge,⁵ and As^{6,7}) and even transition metals^{8,9} (e.g., Nb,^{10,11} Ta,^{10–12} Mo,¹³ W,¹⁴ Re,¹⁵ Fe,¹⁶ Ru,^{17–20} Os,^{21,22} Ni,²³ Pt,²⁴ and

Ir^{25–35}). Recently, examples of a 1,4-phosphoratabenzene³⁶ and an osmabenzene^{37–39} were reported. In addition, metallaromatic complexes have been suggested as intermediates in various reactions.^{15,16,40–42}

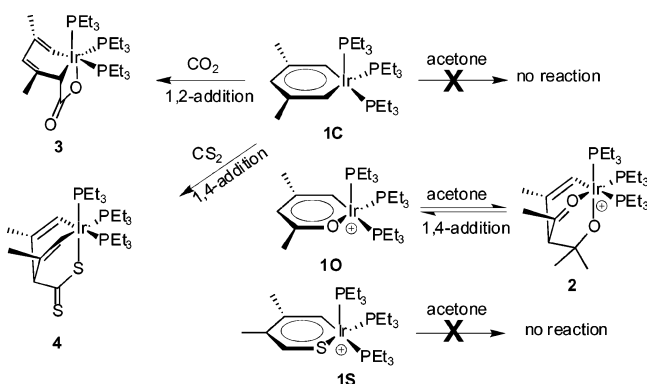
Despite the recent extensive interest in metallabenzene complexes, detailed mechanistic and theoretical investigations into the formation and reactivity of these interesting systems remain remarkably scarce.⁸ Before the first reported isolation

- (1) Kekulé, A. *Bull. Soc. Chim.* **1864**, 3, 98.
- (2) Herberich, G. E.; Englert, U.; Pubanz, D. *J. Organomet. Chem.* **1993**, 459, 1.
- (3) Wakita, K.; Tokitoh, N.; Okazaki, R.; Nagase, S.; von Ragué Schleyer, P.; Jiao, H. *J. Am. Chem. Soc.* **1999**, 121, 11336.
- (4) Baldrige, K. K.; Uzan, O.; Martin, J. M. L. *Organometallics* **2000**, 19, 1477.
- (5) Nakata, N.; Takeda, N.; Tokitoh, N. *J. Am. Chem. Soc.* **2002**, 124, 6914.
- (6) Ashe, A. J., III. *Top. Curr. Chem.* **1982**, 105, 125.
- (7) Elschenbroich, C.; Kroker, J.; Massa, W.; Wunsch, M.; Ashe, A. J., III. *Angew. Chem., Int. Ed. Engl.* **1986**, 25, 571.
- (8) Bleeke, J. R. *Chem. Rev.* **2001**, 101, 1205.
- (9) Bleeke, J. R. *Acc. Chem. Res.* **1991**, 24, 271.
- (10) Riley, P. N.; Profflet, R. D.; Salberg, M. M.; Fanwick, P. E.; Rothwell, I. P. *Polyhedron* **1998**, 17, 773.
- (11) Profflet, R. D.; Fanwick, P. E.; Rothwell, I. P. *Angew. Chem., Int. Ed. Engl.* **1992**, 31, 1261.
- (12) Weller, K. J.; Filippov, I.; Briggs, P. M.; Wigley, D. E. *J. Organomet. Chem.* **1997**, 528, 225.
- (13) Kralik, M. S.; Rheingold, A. L.; Hutchinson, J. P.; Freeman, J. W.; Ernst, R. D. *Organometallics* **1996**, 15, 551.
- (14) Feng, S. G.; White, P. S.; Templeton, J. L. *Organometallics* **1993**, 12, 1765.
- (15) Ferde, R.; Hinton, J. F.; Korfmacher, W. A.; Freeman, J. P.; Allison, N. T. *Organometallics* **1985**, 4, 614.
- (16) Ferde, R.; Allison, N. T. *Organometallics* **1983**, 2, 463.
- (17) Lin, W.; Wilson, S. R.; Girolami, G. S. *Organometallics* **1997**, 16, 2356.
- (18) Liu, S. H.; Ng, W. S.; Chu, H. S.; Wen, T. B.; Xia, H.; Zhou, Z. Y.; Lau, C. P.; Jia, G. *Angew. Chem., Int. Ed.* **2002**, 41, 1589.
- (19) Englert, U.; Podewils, F.; Schiffrers, I.; Salzer, A. *Angew. Chem., Int. Ed.* **1998**, 37, 2134.
- (20) Effertz, U.; Englert, U.; Podewils, F.; Salzer, A.; Wagner, T.; Kaupp, M. *Organometallics* **2003**, 22, 264.
- (21) Elliott, G. P.; Roper, W. R.; Waters, J. M. *J. Chem. Soc., Chem. Commun.* **1982**, 811.
- (22) Rickard, C. E. F.; Roper, W. R.; Woodgate, S. D.; Wright, L. J. *Angew. Chem., Int. Ed.* **2000**, 39, 750.
- (23) Bertling, U.; Englert, U.; Salzer, A. *Angew. Chem., Int. Ed. Engl.* **1994**, 33, 1003.
- (24) Jacob, V.; Weakley, T. J. R.; Haley, M. M. *Angew. Chem., Int. Ed.* **2002**, 41, 3470.
- (25) Chen, J.; Daniels, L. M.; Angelici, R. J. *J. Am. Chem. Soc.* **1990**, 112, 199.
- (26) Gilbertson, R. D.; Weakley, T. J. R.; Haley, M. M. *J. Am. Chem. Soc.* **1999**, 121, 2597.
- (27) Gilbertson, R. D.; Weakley, T. J. R.; Haley, M. M. *Chem.—Eur. J.* **2000**, 6, 437.
- (28) Gilbertson, R. D.; Lau, T. L. S.; Lanza, S.; Wu, H.-P.; Weakley, T. J. R.; Haley, M. M. *Organometallics* **2003**, 22, 3279.
- (29) Bleeke, J. R.; Xie, Y.-F.; Peng, W.-J.; Chiang, M. J. *Am. Chem. Soc.* **1989**, 111, 4118.
- (30) Bleeke, J. R.; Behm, R.; Xie, Y.-F.; Clayton, T. W., Jr.; Robinson, K. D. *J. Am. Chem. Soc.* **1994**, 116, 4093.
- (31) Bleeke, J. R.; Behm, R.; Xie, Y.-F.; Chiang, M. Y.; Robinson, K. D.; Beatty, A. M. *Organometallics* **1997**, 16, 606.
- (32) Bleeke, J. R.; Blanchard, J. M. B. *J. Am. Chem. Soc.* **1997**, 119, 5443.
- (33) Bleeke, J. R.; Blanchard, J. M. B.; Donnay, E. *Organometallics* **2001**, 20, 324.
- (34) Bleeke, J. R.; Hinkle, P. V. *J. Am. Chem. Soc.* **1999**, 121, 595.
- (35) Bleeke, J. R.; Hinkle, P. V. *Organometallics* **2001**, 20, 1939.
- (36) Ashe, A. J., III; Bajko, Z.; Carr, M. D.; Kampf, J. W. *Organometallics* **2003**, 22, 910.
- (37) Wen, T. B.; Zhou, Z. Y.; Jia, G. *Angew. Chem., Int. Ed.* **2001**, 40, 1951.
- (38) Wen, T. B.; Ng, S. M.; Hung, W. Y.; Zhou, Z. Y.; Lo, M. F.; Shek, L.-Y.; Williams, I. D.; Lin, Z.; Jia, G. *J. Am. Chem. Soc.* **2003**, 125, 884.
- (39) For a highlight on osmabenzynes, see: Roper, W. R. *Angew. Chem., Int. Ed.* **2001**, 40, 2440.
- (40) Yang, J.; Jones, W. M.; Dixon, J. K.; Allison, N. T. *J. Am. Chem. Soc.* **1995**, 117, 9776.
- (41) Chin, R. M.; Jones, W. D. *Angew. Chem., Int. Ed. Engl.* **1992**, 31, 357.
- (42) Hughes, R. P.; Trujillo, H. A.; Egan, J. W., Jr.; Rheingold, A. L. *J. Am. Chem. Soc.* **2000**, 122, 2261.

Scheme 1



Scheme 2



of a metallabenzene complex by Roper et al.,²¹ theoretical studies by Thorn and Hoffmann predicted that metallabenzene complexes of Mn and Rh may be viable synthetic targets.⁴³ There are also a few theoretical reports on metallaaromaticity in metal chelate rings⁴⁴ and aromaticity in all-metal clusters.^{45–48} More recently, we communicated on our initial calculations on the reactivity of metallaaromatic iridium complexes toward acetone.⁴⁹

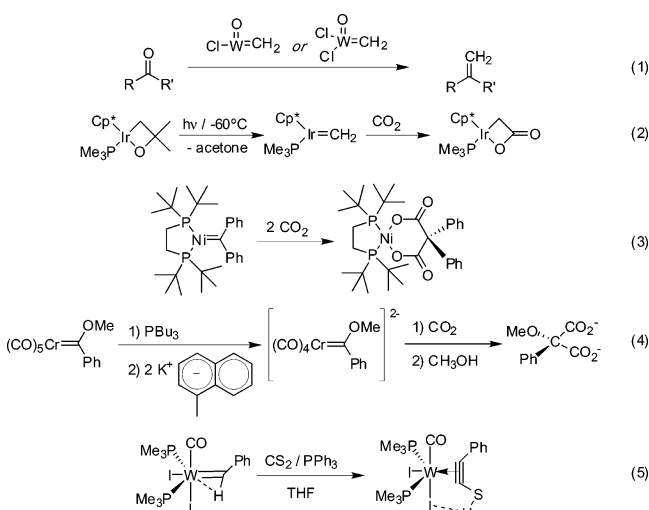
There has been considerable debate whether metallabenzene complexes can be considered aromatic.⁸ The aromatic nature of these complexes is consistent with the Hückel rule ($4n + 2$ π electrons) and molecular orbital calculations.⁴³ The flat metal-organic rings do not show alternating single and double bonds. In addition, their NMR spectra show downfield shifts attributed to aromatic ring currents.³¹ The aromatic nature is also apparent from the observed reactivity. For instance, osmabenzene undergoes electrophilic aromatic substitution much in the same way as benzene (Scheme 1).²²

The cycloaddition reactivity of acetone, CO₂, CS₂, and other substrates with metallabenzene (**1C**),³¹ metallapyrylium (**1O**),³³ and metallathiabenzene (**1S**)³⁵ complexes of iridium reported by Bleeke et al. seems to contrast the aromatic nature (Scheme 2). Remarkably, acetone reacts reversibly with the metallapyrylium complex (**1O**) to give the 1,4-addition product (**2**) but not with the other two complexes (**1C** and **1S**). Furthermore, the metallabenzene complex (**1C**) adds CO₂ in a 1,2-manner (**3**) and the isovalent CS₂ in a 1,4-fashion (**4**). Although these selective addition reactions have been studied in detail, the strikingly different reactivity patterns are not fully understood. The use of transition metals in cycloadditions is common. There are numerous examples where the metal complex participates in the reaction and is one of the reactants and the metal is present

Scheme 3



Scheme 4



in the product.^{50,51} In many cases, they assist in the reaction but are not part of the products.^{52–54}

Formally, the organic moiety of a metallabenzene complex can be viewed as a vinyl carbene ligand (Scheme 3), although experimental and theoretical studies show that these complexes are best considered as aromatic (vide supra).⁸ However, the cycloaddition chemistry might be reminiscent of carbene complexes and of organic alkenes and dienes. A number of related reactions of metallocarbenes with ketones, CO₂, and CS₂ have been reported (Scheme 4). For instance, the tungsten complexes ClW(O)(=CH₂) and Cl₂W(O)(=CH₂) react with ketones and aldehydes to give substituted olefins (eq 1).⁵⁵ The iridium complex Cp*(PMe₃)Ir=CH₂, formed by the photochemical extrusion of acetone from a 2-oxoiridacycle, reacts with CO₂ to give the 1,2-addition product (eq 2).⁵⁶ The similar nickel complex (dtbpe)Ni=CPh₂ reacts with 2 equivalents of CO₂ yielding a six-membered metallacycle (eq 3).⁵⁷ The chromium complex [(CO)₄Cr=CPh(OMe)]²⁻ seems to react with CO₂ in a similar fashion (eq 4).⁵⁸ The tungsten complex (PMe₃)₂I₂(CO)W=CHPh reacts with CS₂ in the presence of PPh₃ to give the η^2 -alkynethiol complex (eq 5).⁵⁹

Density functional theory (DFT) has become a powerful tool in recent years in the investigation of transition metal reactions,^{60,61} especially due to the rapid increase in available computer power and the development of new methods. For example, we have used DFT to investigate H/D scrambling in TpPtMeH₂ (Tp = hydrido-tris-pyrazolylborate),⁶² the rhodium

(43) Thorn, D. L.; Hoffmann, R. *Nouv. J. Chim.* **1979**, *3*, 39.

(44) Masui, H. *Coord. Chem. Rev.* **2001**, *219–221*, 957.

(45) Li, X.; Kuznetsov, A. E.; Zhang, H.-F.; Boldyrev, A. I.; Wang, L.-S. *Science* **2001**, *291*, 859.

(46) Boldyrev, A. I.; Kuznetsov, A. E. *Inorg. Chem.* **2002**, *41*, 532.

(47) Kuznetsov, A. E.; Birch, K. A.; Boldyrev, A. I.; Li, X.; Zhai, H.-J.; Wang, L.-S. *Science* **2003**, *300*, 622.

(48) Tanaka, H.; Neukermans, S.; Jenssens, E.; Silverans, R. E.; Lievens, P. *J. Am. Chem. Soc.* **2003**, *125*, 2862.

(49) Iron, M. A.; Martin, J. M. L.; van der Boom, M. E. *Chem. Commun.* **2003**, 132.

(50) Frühauf, H.-W. *Coord. Chem. Rev.* **2002**, *230*, 79.

(51) Deubel, D. V.; Frenking, G. *Acc. Chem. Res.* **2003**, ASAP, ar020268q.

(52) Lautens, M.; Klute, W.; Tam, W. *Chem. Rev.* **1996**, *96*, 49.

(53) Ojima, I.; Tzamarioudaki, M.; Li, Z.; Donovan, R. *J. Chem. Rev.* **1996**, *96*, 635.

(54) Frühauf, H.-W. *Chem. Rev.* **1997**, *97*, 523.

(55) Kauffmann, T.; Abeln, R.; Welke, S.; Wingbermühle, D. *Angew. Chem., Int. Ed. Engl.* **1986**, *25*, 909.

(56) Klein, D. P.; Bergman, R. G. *J. Am. Chem. Soc.* **1989**, *111*, 3079.

(57) Mindiola, D. J.; Hillhouse, G. L. *J. Am. Chem. Soc.* **2002**, *124*, 9976.

(58) Lee, S.; Cooper, N. J. *J. Am. Chem. Soc.* **1990**, *112*, 9419.

(59) Lee, T.-Y.; Mayr, A. *J. Am. Chem. Soc.* **1994**, *116*, 10300.

(60) Niu, S.; Hall, M. B. *Chem. Rev.* **2000**, *100*, 353.

(61) Ziegler, T. In *Computational Thermochemistry Prediction and Estimation of Molecular Thermodynamics*; Irikura, K. K., Frurip, D. J., Eds.; American Chemical Society: Washington, DC, 1998; pp 369–382.

catalyzed hydrogenation of acetone,⁶³ the palladium catalyzed Heck reaction,⁶⁴ stabilization strategies of silanones,^{65,66} and C–H versus C–C bond activation by rhodium complexes.^{67–69} The challenge here is clear: is it possible by means of DFT to develop a fundamental understanding of the rather complex metalloaromatic chemistry? Here, we use DFT calculations to elucidate the mechanistic aspects of the intriguing cycloaddition reactions of acetone, CO₂, and CS₂ to the iridium metalloaromatic complexes [(C₄H₄YIr)(PH₃)₃]ⁿ⁺ (**5C**, Y = CH, *n* = 0; **5O**, Y = O, *n* = +1; **5S**, Y = S, *n* = +1) and their rhodium analogues **5***.

Computational Details

All calculations were carried out using Gaussian 98 revision A11.⁷⁰ The mPW1K (modified Perdew–Wang 1-parameter for kinetics) DFT exchange–correlation functional of Truhlar and co-workers⁷¹ was used to investigate the reactions. This functional is based on the Perdew–Wang exchange functional⁷² with Adamo and Barone’s modified enhancement factor⁷³ and the Perdew–Wang correlation functional.⁷² A larger percentage of Hartree–Fock exchange has been introduced⁷¹ to circumvent the underestimated barrier heights typical of standard exchange–correlation functionals. It has been shown (e.g., refs 62, 71, 74, 75) that this functional generally yields much more reliable reaction barrier heights than B3LYP or other “conventional” exchange–correlation functionals.

With this functional, two basis set–RECP (relativistic effective core potential) combinations were used. The first, denoted SDD, is the combination of the Huzinaga–Dunning double- ζ basis set on lighter elements with the Stuttgart–Dresden basis set–RECP combination⁷⁶ on transition metals. The second, denoted SDB-cc-pVDZ, combines the Dunning cc-pVDZ basis set⁷⁷ on the main group elements and the Stuttgart–Dresden basis set–RECP on the transition metals with an added *f*-type polarization exponent taken as the geometric average of the two *f*-exponents given in the Appendix to ref 78. Geometry optimizations were carried out using the former basis set, while the energetics of the reaction were calculated at these geometries with the

latter basis set; this level of theory is conventionally denoted as mPW1K/SDB-cc-pVDZ//mPW1K/SDD. We have previously recommended this level of theory as better suited than the more popular B3LYP^{79,80}/LANL2DZ⁸¹ to investigate reaction mechanisms.⁶²

The identities of the transition states were confirmed by having only one imaginary vibrational mode suitable for the desired reaction. In addition, an intrinsic reaction coordinate (IRC) calculation was performed on each transition state to confirm connectivity with the reactant(s) and the product.^{82–84}

Bulk solvation effects⁸⁵ were approximated by single-point mPW1K/SDB-cc-pVDZ energy calculations using a polarized continuum (overlapping spheres) model (PCM).^{86–88} Either acetone ($\epsilon = 20.7$)⁷⁰ or tetrahydrofuran ($\epsilon = 7.58$)⁷⁰ was used depending on the solvent used in the experimental procedures.^{31,33,35} Energies at this level of theory are denoted PCM/mPW1K/SDB-cc-pVDZ//mPW1K/SDD.

Since Gaussian 98 uses the same number of radial grid points throughout the periodic table, the “ultrafine” grid, that is, a pruned (99,590) grid, was used throughout the calculations as recommended in ref 89. Nevertheless, due to the size of the systems with PMe₃ ligands (vide infra), such a grid makes the calculations far too computationally expensive and the default grid, that is, a pruned (75,302) grid, was used for the mPW1K/SDD geometry optimizations and the ultrafine grid for the mPW1K/SDB-cc-pVDZ single-point energy calculations, both in the gas phase calculations and with the PCM model. Likewise, the lengthy IRC calculations were carried out using the default integration grids.

Results and Discussion

The following naming scheme will be used hereinafter for the calculated complexes and transition states. Each complex is assigned a name comprised of three components: its place in the reaction profile (a number, **5–10**), type of metalloaromatic ring (**C** = metallabenzene, **O** = metallaopyrylium, **S** = metalla-thiabenzene), and the type of adduct formed (**a** = acetone, **o** = CO₂, **s** = CS₂). Transition states are labeled according to the two minima they connect. The two aromatic methyl groups are present in the experimental complexes (**1C**, **1O**, and **1S**; Scheme 2) due to synthetic requirements but are not expected to dramatically affect their reactivity and, therefore, are replaced by hydrogens in the calculations. Likewise, the bulky PEt₃ ligands are replaced by the smaller PH₃.

Geometries. Selected complexes are depicted in Figure 1 and all are presented in the Supporting Information. The iridiaaromatic complexes (**5**) are square pyramidal complexes with apical phosphine ligands and basically flat rings.⁹⁰ The agreement is satisfactory between the structures of **5C** and **5O** and the X-ray structures of **1C**³¹ and **1S**,³⁴ respectively.⁹¹ In these calculated complexes, there is minimal variation in the aromatic C–C bond lengths, which are around the calculated bond lengths for

- (62) Iron, M. A.; Lo, H. C.; Martin, J. M. L.; Keinan, E. *J. Am. Chem. Soc.* **2002**, *124*, 7041.
 (63) Iron, M. A.; Sundermann, A.; Martin, J. M. L. *J. Am. Chem. Soc.* **2003**, ASAP, ja028489e.
 (64) Sundermann, A.; Uzan, O.; Martin, J. M. L. *Chem.–Eur. J.* **2001**, *7*, 1703.
 (65) Uzan, O.; Martin, J. M. L. *Chem. Phys. Lett.* **1998**, *290*, 535.
 (66) Uzan, O.; Gozin, Y.; Martin, J. M. L. *Chem. Phys. Lett.* **1998**, *288*, 356.
 (67) Sundermann, A.; Uzan, O.; Milstein, D.; Martin, J. M. L. *J. Am. Chem. Soc.* **2000**, *122*, 7095.
 (68) Sundermann, A.; Uzan, O.; Martin, J. M. L. *Organometallics* **2001**, *20*, 1703.
 (69) Rytchinski, B.; Oevers, S.; Montag, M.; Vignalok, A.; Rozenberg, H.; Martin, J. M. L.; Milstein, D. *J. Am. Chem. Soc.* **2001**, *123*, 9064.
 (70) Frisch, M. J.; Trucks, G. W.; Schlegel, H. B.; Scuseria, G. E.; Robb, M. A.; Cheeseman, J. R.; Zakrzewski, V. G.; Montgomery, J. A.; Stratmann, R. E.; Burant, J. C.; Dapprich, S.; Millam, J. M.; Daniels, A. D.; Kudin, K. N.; Strain, M. C.; Farkas, O.; Tomasi, J.; Barone, V.; Cossi, M.; Cammi, R.; Mennucci, B.; Pomelli, C.; Adamo, C.; Clifford, S.; Ochterski, J.; Petersson, G. A.; Ayala, P. Y.; Cui, Q.; Morokuma, K.; Salvador, P.; Dannenberg, J. J.; Malick, D. K.; Rabuck, A. D.; Raghavachari, K.; Foresman, J. B.; Cioslowski, J.; Ortiz, J. V.; Baboul, A. G.; Stefanov, B. B.; Liu, G.; Liashenko, A.; Piskorz, P.; Komaromi, I.; Gomperts, R.; Martin, R. L.; Fox, D. J.; Keith, T.; Al-Laham, M. A.; Peng, C. Y.; Nanayakkara, A.; Challacombe, M.; Gill, P. M. W.; Johnson, B.; Chen, W.; Wong, M. W.; Andres, J. L.; Gonzalez, C.; Head-Gordon, M.; Replogle, E. S.; Pople, J. A. Gaussian 98, revision A.11; Gaussian Inc.: Pittsburgh, PA, 2001.
 (71) Lynch, B. J.; Fast, P. L.; Harris, M.; Truhlar, D. G. *J. Phys. Chem. A* **2000**, *104*, 4811.
 (72) Perdew, J. P.; Chevary, J. A.; Vosko, S. H.; Jackson, K. A.; Perderson, M. R.; Singh, D. J.; Fiolhais, C. *Phys. Rev. B* **1992**, *46*, 6771.
 (73) Adamo, C.; Barone, V. *J. Chem. Phys.* **1998**, *108*, 664.
 (74) Lynch, B. J.; Truhlar, D. G. *J. Phys. Chem. A* **2001**, *105*, 2936.
 (75) Parthiban, S.; de Oliveira, G.; Martin, J. M. L. *J. Phys. Chem. A* **2001**, *105*, 895.
 (76) Dolg, M. In *Modern Methods and Algorithms of Quantum Chemistry*; Grotendorst, J., Ed.; John von Neumann Institute for Computing, Jülich, 2000; Vol. 1, pp 479–508.
 (77) Dunning, T. H., Jr. *J. Chem. Phys.* **1989**, *90*, 1007.
 (78) Martin, J. M. L.; Sundermann, A. *J. Chem. Phys.* **2001**, *114*, 3408.

- (79) Becke, A. D. *J. Chem. Phys.* **1993**, *98*, 5648.
 (80) Stevens, P. J.; Devlin, F. J.; Chabalowski, C. F.; Frisch, M. J. *J. Phys. Chem.* **1994**, *98*, 11623.
 (81) Hay, P. J.; Wadt, W. R. *J. Chem. Phys.* **1985**, *82*, 299.
 (82) Fukui, K. *Acc. Chem. Res.* **1981**, *14*, 363.
 (83) Gonzalez, C.; Schlegel, H. B. *J. Chem. Phys.* **1989**, *90*, 2154.
 (84) Gonzalez, C.; Schlegel, H. B. *J. Phys. Chem.* **1990**, *94*, 5523.
 (85) Cramer, C. J. In *Essentials of Computational Chemistry: Theories and Models*; John Wiley & Sons: Chichester, U.K., 2002; pp 347–383.
 (86) Miertus, S.; Scrocco, E.; Tomasi, J. *J. Chem. Phys.* **1981**, *55*, 117.
 (87) Miertus, S.; Tomasi, J. *J. Chem. Phys.* **1982**, *65*, 239.
 (88) Cossi, M.; Barone, V.; Cammi, R.; Tomasi, J. *J. Chem. Phys. Lett.* **1996**, *255*, 327.
 (89) Martin, J. M. L.; Bauschlicher, C. W., Jr.; Ricca, A. *Comput. Phys. Commun.* **2001**, *133*, 189.
 (90) The structure of the metallaaromatic complexes are square planar but show fast phosphine exchange as evident from the ³¹P {¹H} NMR spectrum; see ref 31.
 (91) The X-ray structure of **1O** was not reported; see ref 32.

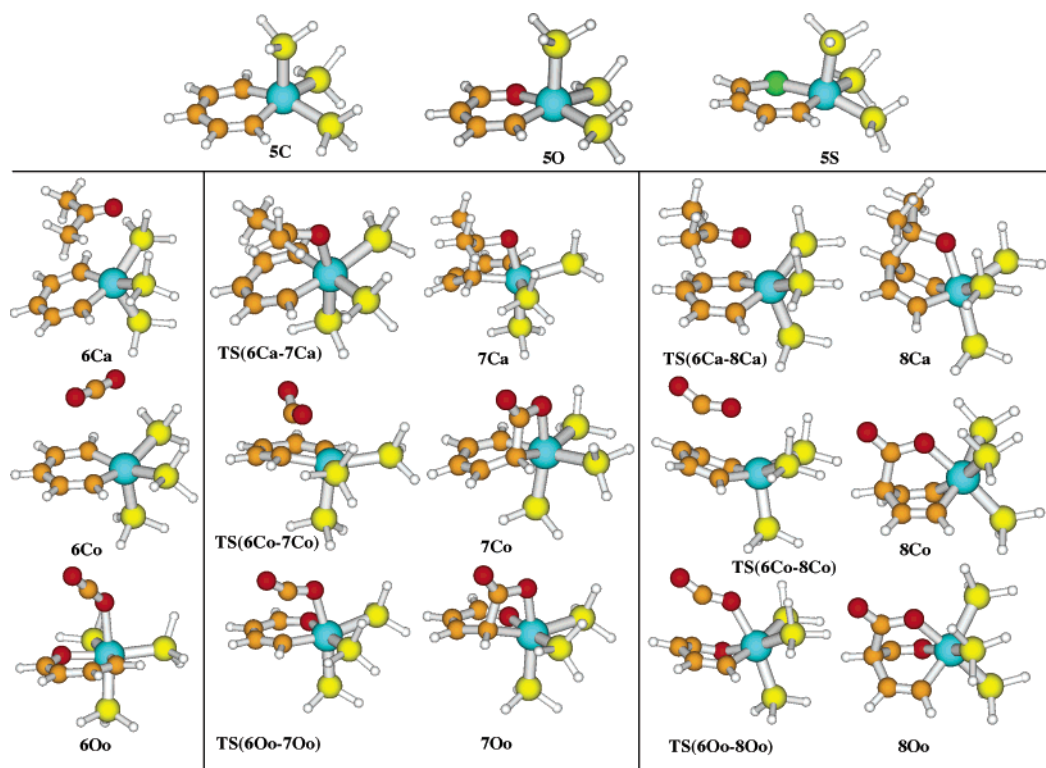
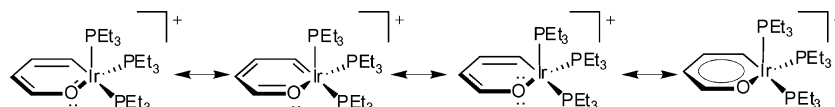


Figure 1. Selected calculated geometries. (Top) Metalloaromatic complexes; (left) substrate complexes; (center) 1,2-addition; (right) 1,4-addition. (Color scheme: C, brown; H, white; Ir, cyan; O, red; P, yellow; S, green.)

Scheme 5



benzene of 1.396 Å. In fact, the $C_{\text{ortho}}-C_{\text{meta}}$ and $C_{\text{meta}}-C_{\text{para}}$ bond lengths in **5C** are 1.395 and 1.398 Å, respectively, in line with expectations for an aromatic system. Phosphine dissociation from **5** was examined and found not to occur (*vide infra*).

The next step is the substrate coordination ($L = \text{acetone}, \text{CO}_2$, or CS_2) to the iridium center to afford $[(\text{C}_4\text{H}_4\text{YIr})(\text{L})(\text{PH}_3)_3]^{n+}$ (**6**). Two types of coordination complexes were found. The cationic **5O** and **5S** form η^1 -complexes. Upon coordination, a pattern of alternating C–C and C=C bonds emerges in the metal–ring system (similar in lengths as in the 1,2- and 1,4-addition products **7O** and **7S**; *vide infra*), suggesting loss of aromaticity and formation of a cyclohexadiene-like structure. The ring bond lengths are similar within each set of three coordination complexes (**6Oaos** and **6Saos**). The formation of the substrate coordination complexes is made possible by an additional resonance structure that allows for the chalcogen to accept electron density preventing the formation of formally 20-electron complexes (Scheme 5).³³ Indeed it is known that complexes **1O** and **1S** (Scheme 2) react with PMe_3 to give the hexacoordinate complexes $[(\text{Me}_2\text{H}_2\text{C}_4\text{Y})\text{Ir}(\text{PMe}_3)_4]^+$ ($Y = \text{O}^{33}$ or S^{35}). With the iridiabenzene complex (**1C**, $Y = \text{C}$), only the tris- PMe_3 complex is obtained.³¹

The calculated Ir–O(acetone) bond distances in **6Oa** and **6Sa** are 2.131 and 2.140 Å, respectively. These values are in the same range as in other X-ray characterized Ir–O(acetone) complexes (2.127(6) Å and 2.185(4) Å).^{92,93} The ring Ir–O distances in complexes **5O** and **6Oa** are 1.997 and 2.030 Å,

respectively, which are significantly shorter than the Ir–O(acetone) distances, thereby emphasizing the aromatic nature of these complexes. In the acetone coordination complexes **6Oa** and **6Sa**, the C=O bond of acetone has lengthened from 1.235 Å (calculated for free acetone at the same level of theory) to 1.256 Å, consistent with the abovementioned crystallographically characterized Ir-acetone complexes (C=O: 1.248(10) Å and 1.232(7) Å).^{92,93} The analogous CO_2 (**6Oo** and **6So**) and CS_2 (**6Os** and **6Ss**) coordination complexes are structurally similar. In these complexes, the C=X–Ir double bond ($X = \text{O}, \text{S}$) of the incoming substrate has lengthened compared to calculated double bond lengths in free CX_2 while the uncoordinated C=X bond has shortened, consistent with electron donation to the metal center. Meanwhile, the X=C=X angle remains nearly linear (178.5° in **6So**, 178.6° in **6Oo** and **6Os**, and 179.3° in **6Ss**).

A resonance structure where electron density is localized on the carbon ortho to the iridium center is not favorable with **5C**, and indeed substrate coordination does not occur. Instead, in **6C** the incoming substrate hovers above the ring forming a long-range complex and does not coordinate to the metal center. The metallabenzene moiety remains unaffected (changes in ring C–C bond lengths are <0.002 Å). The bond lengths in the substrate are likewise not substantially different from those in

(92) Jiménez, M. V.; Sola, E.; López, J. A.; Lahoz, F. J.; Oro, L. A. *Chem.–Eur. J.* **1998**, *4*, 1398.

(93) Lee, D.-H.; Chen, J.; Faller, J. W.; Crabtree, R. H. *Chem. Commun.* **2001**, 213.

the free substrate, and the $X=C=X$ angles remain linear (175.5° in **6Co** and 179.9° in **6Cs**).

The products of 1,2- and 1,4-cycloaddition (**7** and **8**, respectively) were identified, and their geometries exhibit the expected distinct single and double bonds. Complex **7** has a 1-iridia-2,4-cyclohexadiene-like core, whereas **8** has a 1-iridia-2,5-cyclohexadiene-like core. This is apparent in the shorter single and longer double bonds than in **8** where the double bonds are not conjugated. In the CX_2 cycloaddition products ($X = O, S$), the $X=C-X$ angles are in the expected range of $\sim 121^\circ$ – 128° . The calculated structure of **7Co** compares satisfactorily with the reported X-ray crystal structure of **3**.³⁰

These cycloaddition reactions may either follow a concerted (i.e., Diels–Alder) or nonconcerted reaction pathway. The metallabenzene complex (**5C**) reacts with all three substrates in a concerted fashion, and the C–C and Ir–X ($X = O, S$) bonds are formed simultaneously. This is apparent from the transition states found, **TS(6C-7C)** for 1,2-addition and **TS(6C-8C)** for 1,4-addition, where both the Ir–X ($X = O, S$) and the C–C bonds are formed in one concerted step. The other two complexes (**5O** and **5S**) react with the substrates in a nonconcerted manner, and a substrate coordination complex (**6O** or **6S**) is formed prior to C–C bond formation. From the coordination complex, there is a transition state for C–C bond formation.

The transition state for 1,4-cycloaddition, **TS(6-8)**, has the ring C_{para} bent toward the substrate carbon atom, which likewise is bent toward the ring. In the additions of CX_2 ($X = O, S$), the $X=C-X$ angle is $\sim 147^\circ$ – 157° , intermediate between the reactants ($\sim 180^\circ$) and the products ($\sim 125^\circ$). The 1,2-cycloaddition transition states, **TS(6Cos-7Cos)**, for the addition of CX_2 ($X = O, S$) have the substrate aligned perpendicular to the Ir– C_{ortho} bond. The CX_2 substrate rotates during the reaction to form the cycloaddition product, as confirmed by IRC calculations (see Computational Details section). Such a transition state is expected from orbital considerations (vide infra). For acetone, such a transition state could not be found, probably because the greater bulk of the acetone substrate makes it more difficult to rotate. In this case, the transition state, **TS(6Ca-7Ca)**, is like that for the 1,4-addition where the substrate is aligned parallel to the Ir– C_{ortho} bond.

Reaction Energies. The calculated energies of the various complexes relative to **5** + L ($L = \text{acetone, CO}_2, \text{ or CS}_2$) are presented in Table 1. From these results, one can clearly understand the observed experimental reactivity (Scheme 2).^{31,33,35} The reaction of the metallapyrylium complex (**5O**) with acetone leads to reversible formation of the 1,4-addition product **8Oa**. Here, the formation of the acetone complex (**6Oa**) is exergonic. The addition barrier, **TS(6Oa-8Oa)**, is relatively low ($\Delta G_{298}^\ddagger = 14.5$ kcal/mol), and the addition is almost thermoneutral ($\Delta G_{298} = 1.2$ kcal/mol). The experimentally unobserved 1,2-addition reaction of **5O** with acetone has a higher reaction barrier ($\Delta G_{298}^\ddagger = 18.9$ kcal/mol) and is endergonic ($\Delta G_{298} = 7.1$ kcal/mol). The other two metalloaromatic complexes (**5C** and **5S**) are known not to react with acetone.^{31,35,94} Even though the calculated reaction barriers for the reaction of **5S** with acetone are not too high ($\Delta G_{298}^\ddagger = 23.4$ kcal/mol for 1,4-addition and

Table 1. Calculated Relative Energies (kcal/mol) of Complexes **5–8** and **10**

	+ acetone (a)		+ CO ₂ (o)		+ CS ₂ (s)	
	ΔE_0	ΔG_{298}	ΔE_0	ΔG_{298}	ΔE_0	ΔG_{298}
5C/5O/5S	0.0	0.0	0.0	0.0	0.0	0.0
6C	−6.7	3.3	−3.9	4.3	−1.6	6.2
TS(6C-7C)	27.4	41.9	21.8	33.8	20.4	33.8
7C	−13.1	4.7	−11.5	1.8	−35.1	−21.6
TS(6C-8C)	18.6	33.2	28.3	39.0	16.5	28.1
8C	−17.8	−0.2	−12.2	2.4	−35.3	−20.8
10C + PH ₃	31.2	20.1	34.1	19.8	31.6	17.2
6O	−22.5	−7.9	−1.3	8.8	−4.7	5.9
TS(6O-7O)	−4.1	11.0	9.2	20.1	2.0	12.7
7O	−18.2	−0.8	−6.4	5.8	−30.4	−16.6
TS(6O-8O)	−9.5	6.6	8.2	20.0	0.3	12.1
8O	−24.4	−6.7	−7.8	6.3	−28.2	−14.3
10O + PH ₃	26.0	11.6	26.2	12.9	25.3	11.7
6S	−21.9	−7.6	−1.4	8.9	−5.1	5.7
TS(6S-7S)	2.8	18.6	14.5	25.4	5.8	16.3
7S	−5.1	12.1	5.2	17.6	−17.2	−3.6
TS(6S-8S)	−0.2	15.8	15.3	27.0	5.8	17.4
8S	−9.8	6.7	5.8	19.5	−15.3	−1.7
10S + PH ₃	31.5	16.9	29.8	15.7	38.2	25.3

$\Delta G_{298}^\ddagger = 26.2$ kcal/mol for 1,2-addition), the overall reactions are endergonic. The metallabenzene complex (**5C**) is unreactive toward acetone as it involves excessive barriers ($\Delta G_{298}^\ddagger = 33.2$ kcal/mol for 1,4-addition and $\Delta G_{298}^\ddagger = 41.9$ kcal/mol for 1,2-addition).

The additions of CO₂ and CS₂ to the metallabenzene complex (**5C**) lead to the 1,2-addition (**7Co**) and 1,4-addition (**8Cs**) products, respectively. These two reactions are not expected to be reversible. The addition of CO₂ has reaction barriers of $\Delta G_{298}^\ddagger = 33.8$ kcal/mol for 1,2-addition and $\Delta G_{298}^\ddagger = 39.0$ kcal/mol for 1,4-addition. These barriers include both the transition state and the formation of the CO₂ complex because the latter is endergonic due to loss of entropy. CS₂ adds in a 1,4-manner to **5C** as, in this case, this barrier is lower ($\Delta G_{298}^\ddagger = 28.1$ versus 33.8 kcal/mol) and this reaction is quite exergonic ($\Delta G_{298} = -20.8$ kcal/mol).

While the gas phase computational results are fairly satisfactory, there are some minor discrepancies. For instance, the addition of acetone to the metallapyrylium (**5O**) is slightly endergonic (**8Oa** compared to **6Oa**), yet when an acetone solution of **10** is cooled to -40°C , the 1,4-addition product (**2**) is clearly detected by NMR. At room temperature, broad peaks are observed.³³ The barrier of the CO₂ 1,2-addition to **5C** ($\Delta G_{298}^\ddagger = 33.8$ kcal/mol) is a bit too high for the reaction to proceed at room temperature, and the reaction is slightly endergonic ($\Delta G_{298} = 1.8$ kcal/mol). At the same time, the barrier for 1,4-addition of acetone to **5C** is $\Delta G_{298}^\ddagger = 33.2$ kcal/mol, and this reaction is not reported experimentally. These issues are resolved when the bulk solvent effects are taken into account, as shown in Table 2, using the PCM solvation model (vide supra Computational Details). The addition of acetone to **5O** is now calculated to be slightly exergonic ($\Delta G_{298} = -1.0$ kcal/mol) in agreement with experimental observations.³³ Furthermore, the addition of CO₂ to **5C** has a barrier of $\Delta G_{298}^\ddagger = 24.3$ kcal/mol and is exergonic ($\Delta G_{298} = -4.0$ kcal/mol). The barrier for acetone 1,4-addition is $\Delta G_{298}^\ddagger = 37.6$ kcal/mol, and thus this reaction is not expected to occur.

The good agreement between the calculated (Table 2) and reported (Scheme 2) reactions allows an estimation of the

(94) While it is not explicitly mentioned that the metallabenzene and metallathiabenzene complexes do not react with acetone, the NMR spectra are reported in this solvent; see refs 30 and 34.

Table 2. Calculated Relative Free Energies (ΔG_{298} , kcal/mol), Including Bulk Solvent Effects, of the Calculated Complexes **5–8** and **10**

	+ acetone (a)	+ CO ₂ (o)	+ CS ₂ (s)
5C/5O/5S	0.0	0.0	0.0
6C	9.5	7.7	11.4
TS(6C-7C)	45.6	24.3	29.0
7C	8.2	-4.0	-24.8
TS(6C-8C)	37.6	37.4	27.1
8C	3.8	-2.6	-24.9
10C + PH₃	21.0	20.9	18.6
<hr/>			
6O	-6.7	10.1	8.2
TS(6O-7O)	10.7	19.8	14.4
7O	-2.7	0.6	-19.5
TS(6O-8O)	7.0	19.2	13.0
8O	-7.6	0.8	-18.4
10O + PH₃	11.8	12.8	12.1
<hr/>			
6S	-6.0	9.8	8.1
TS(6S-7S)	18.2	24.8	17.8
7S	10.1	12.3	-7.6
TS(6S-8S)	15.9	26.0	17.8
8S	6.5	14.9	-5.0
10S + PH₃	16.3	16.1	25.7

product distribution of the following four similar hypothetical reactions. The reaction of CO₂ with the metallathiabenzene (**5S**) is unlikely to occur as both 1,2- and 1,4-additions are fairly endergonic ($\Delta G_{298} = 12.3$ and 14.9 kcal/mol, respectively). In the reaction of the metallapyrylium complex (**5O**) with CO₂, both 1,2- and 1,4-additions are thermoneutral ($\Delta G_{298} = 0.6$ and 0.8 kcal/mol, respectively) and both reaction barriers ($\Delta G_{298}^{\ddagger} = 19.8$ and 19.2 kcal/mol, respectively) are of similar heights. Therefore, one can expect a mixture of both CO₂ addition products and unreacted starting material. The reactions of CS₂ with both complexes (**5O** and **5S**) are exergonic ($\Delta G_{298} = -19.5$ and -18.4 kcal/mol, respectively, for **5O** and **5S**) and again, in each case, involve barriers of similar height ($\Delta G_{298}^{\ddagger} = 14.4$ and 13.0 kcal/mol, respectively, for **5O** and $\Delta G_{298} = 17.8$ kcal/mol for **5S**). Thus, again one might expect nonselective reactions; however, this has not been verified experimentally.

To check the possibility of phosphine dissociation playing a part in the cycloaddition reactions, the complexes *cis*-[(C₄H₄-YIr)(PH₃)₂]ⁿ⁺ (**9**) were optimized. The dissociation of the third phosphine is highly endergonic in all three cases, even when solvent effects are considered (PCM model, see Computational Details) with $\Delta G_{298} = 18.6$ (**9C**), 17.4 (**9O**), and 16.3 kcal/mol (**9S**). The reported exchange of one PEt₃ ligand in **1C** with PMe₃ proceeded via a dissociative mechanism with a rate-determining phosphine dissociation step of $\Delta G_{298}^{\ddagger} = 23$ kcal/mol.³¹ In a similar manner, phosphine dissociation for the coordination complexes **6** to give complexes **10** is also fairly endergonic (see Tables 1 and 2).

Effect of the PMe₃ Ligands. To determine the effect of substituting the PEt₃ with the model PH₃ ligands, some of the reactions were re-examined using PMe₃ ligands; using the ethyl analogue would be far too computationally demanding. The structures involved in the additions of acetone to all three PMe₃ complexes (**5'**) and of CO₂ to the metallabenzene complex (**5C'**) were reoptimized, and the results are presented in Table 3. In general, the outcome obtained using both PH₃ and PMe₃ are similar. One significant difference is that the formation of the coordination complexes **6O'** and **6S'** is no longer exergonic.

Table 3. Calculated Gas-Phase and Solution (PCM) Relative Energies (kcal/mol) of the PMe₃ Complexes **5'–8'**

	5C' + acetone		5O' + acetone		5S' + acetone		5C' + CO ₂	
	gas phase	PCM	gas phase	PCM	gas phase	PCM	gas phase	PCM
5'	0.0	0.0	0.0	0.0	0.0	0.0	0.0	0.0
6'	4.5	14.4	0.5	4.8	4.6	9.4	7.6	17.2
TS(6'-7')	45.7	51.1	17.3	22.0	26.9	30.7	28.1	29.2
7'	6.6	11.7	6.5	9.1	20.3	23.4	-4.5	-2.4
TS(6'-8')	28.1	34.8	9.8	15.1	18.3	24.3	31.8 ^a	36.3 ^a
8'	-6.7	-0.8	-2.6	0.4	10.7	14.5	-5.7	-4.3

^a A fully optimized mPWIK/SDD structure was not found. Reported values are calculated mPWIK/SDB-cc-pVDZ single-point energies at the minimum energy structure obtained during the optimization. A vibrational frequencies calculation resulted in only one imaginary frequency, apropos for a transition state structure.

This may be due to steric interaction with the larger phosphine ligand. In **6Oa** and **6Os** there might be a weak interaction between the acetone and the apical PH₃, yet this does not have a significant impact on the reaction barriers. The barrier for 1,4-addition of acetone to the metallapyrylium complex (**5O'**) is now $\Delta G_{298}^{\ddagger} = 15.1$ kcal/mol instead of 13.7 kcal/mol. Moreover, the unobserved 1,2-addition barrier has increased to $\Delta G_{298}^{\ddagger} = 22.0$ kcal/mol, making this reaction even more unfavorable.

Reactivity. Several factors influencing the reactivity of **5** have been identified. These include the type of reaction mechanism (concerted versus nonconcerted), orbital symmetry considerations, size of the electrophile, and geometry of the reaction product.

The metallabenzene complex (**5C**) reacts via a concerted mechanism, as evident from the substrate complexes **6C** where the substrate “lies” above the aromatic ring, and the transition states where both the Ir–X (X = O, S) and the C–C bonds are formed simultaneously in one step. The metallapyrylium (**5O**) and metallathiabenzene (**5S**) complexes react via a nonconcerted mechanism. They are cationic, unlike **5C**, and are stabilized by coordination of the electronegative O or S. The formation of these coordination complexes is facilitated by the resonance structure of **5O** and **5S** where electron density can be localized on the chalcogen atom (Scheme 5, vide supra). The formation of all nine coordination complexes (**6**) is exoenergetic, but loss of entropy makes the formation of most of them endergonic (i.e., on the G₂₉₈ surface; see Table 2). The addition of acetone has a greater effect on the coordination energy than the linear CX₂ (X = O, S) substrates, possibly because it has a dipole moment.

The frontier orbitals of **5C**, **5O**, acetone, and CO₂ are illustrated in Figure 2; those of **5S** and CS₂ are similar to **5O** and CO₂, respectively. If one examines those of acetone, CO₂, and CS₂, one can clearly see that the reaction is an electrophilic attack of the substrate on the aromatic ring. The HOMO (highest occupied molecular orbital) of acetone is contained within the molecular plane, but the reaction with the metalloaromatic ring transpires perpendicular to this plane. The LUMO (lowest unoccupied molecular orbital) of acetone is the C=O π^* orbital and, hence, is perpendicular to the molecular plane and is antisymmetric (i.e., + on C and – on O). Likewise, the HOMOs of CO₂ and CS₂ do not have any contributions from the carbon atoms and thus cannot interact with the metalloaromatic complexes, while the LUMO, which is antisymmetric with

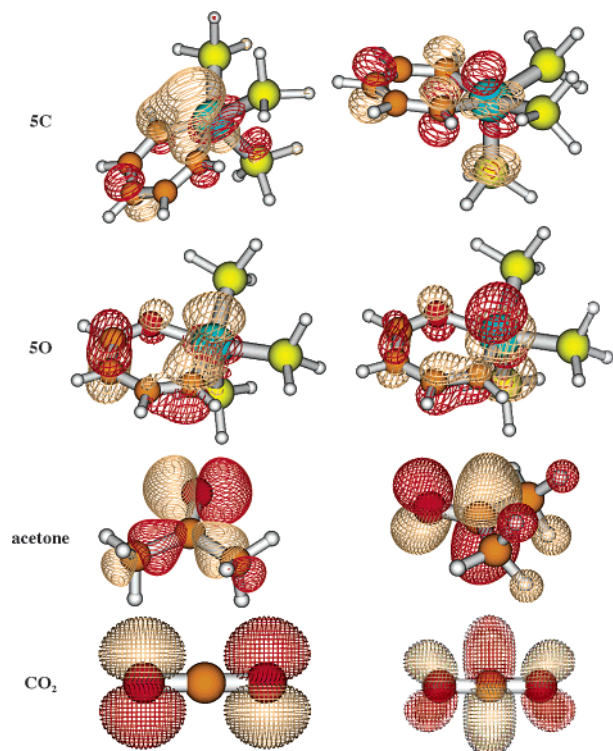


Figure 2. Frontier orbitals of **5C**, **5O**, acetone, and CO_2 (left, HOMO; right, LUMO). See Figure 1 for atomic color scheme.

respect to the C and the O/S atoms, can. Moreover, the symmetry of the metalloaromatic HOMO and the electrophile LUMO have the appropriate orbital symmetries for 1,4-addition. This is expected as this is a [4 + 2] electron cycloaddition reaction, and the Woodward–Hoffmann rules⁹⁵ predict such a reaction to be symmetry allowed. In addition, it is apparent that the 1,2-addition reaction is symmetry forbidden, although this does not preclude it from occurring.

The orbital symmetry also explains the geometry of **TS(6Co-7Co)**. It is observed experimentally that CO_2 reacts with the metallabenzene complex to give a 1,2-addition product.³¹ Because the HOMO of **5C** (vis-à-vis the Ir and C_{ortho} centers) and the LUMO of CO_2 have different symmetries, the CO_2 cannot approach parallel to the Ir– C_{ortho} bond, and thus the perpendicular transition state is obtained. In this reaction, first an interaction occurs between the carbon of CO_2 and C_{ortho} of **5C** and then the CO_2 rotates to form the Ir–O bond, all in one concerted step. A similar transition state is obtained for the 1,2-addition of CS_2 to **5C**.

Another factor affecting reactivity is the length of the electrophile $\text{C}=\text{X}$ ($\text{X} = \text{O}$ or S) bond. The 1,4-addition requires this double bond to stretch across the metalloaromatic ring. The more stretching required, the less favorable the overall process. The calculated $\text{C}=\text{X}$ bond lengths in free CO_2 , acetone, and CS_2 are 1.178, 1.235, and 1.576 Å, respectively. For the 1,4-addition, these bonds have to stretch across the Ir $\cdots\text{C}_{\text{para}}$ diagonal, which are 3.400 Å (**5O**), 3.465 Å (**5C**), and 3.602 Å (**5S**). This Ir $\cdots\text{C}_{\text{para}}$ diagonal is another parameter influencing reactivity. These factors are clearly observable in the various reported reactions. The smallest electrophile, CO_2 , would rather react with **5C** in a symmetry forbidden 1,2-manner than stretch

Table 4. Calculated Gas Phase and Solution (PCM) Relative Energies (ΔG_{298}) of the Rhodium Complexes **5***–**8***

	+ acetone (a)		+ CO_2 (o)		+ CS_2 (s)	
	gas phase	PCM	gas phase	PCM	gas phase	PCM
5C* / 5O* / 5S*	0.0	0.0	0.0	0.0	0.0	0.0
6C*	4.1	10.3	4.4	7.9	6.3	11.9
TS(6C*-7C*)	36.5	40.0	26.6	23.4	31.7	28.0
7C*	3.1	5.1	−0.8	−7.0	−22.5	−26.0
TS(6C*-8C*)	31.0	35.5	36.3	35.2	27.3	26.5
8C*	0.8	4.8	2.6	−2.9	−19.4	−23.7
6O*	−7.6	1.6	6.9	8.3	6.2	8.6
TS(6O*-7O*)	7.9	16.8	20.4	19.9	15.1	16.6
7O*	−4.4	2.7	6.6	1.3	−15.8	−18.6
TS(6O*-8O*)	7.9	12.5	19.9	19.0	14.6	15.2
8O*	−4.4	0.0	8.0	2.5	−11.5	−15.5
6S*	−7.5	−0.9	6.4	7.6	5.4	8.1
TS(6S*-7S*)	19.6	23.9	25.7	25.1	19.0	20.8
7S*	13.0	15.7	18.5	12.7	−2.9	−6.4
TS(6S*-8S*)	17.3	22.0	22.4	18.1	19.8	20.3
8S*	10.4	15.2	21.7	17.4	1.5	−1.5

across the ring. With the smaller **5O**, both reactions have similar barriers but are thermoneutral. The reaction of CO_2 with **5S** is not expected to occur. The largest electrophile, CS_2 , can react with all three complexes (**5COS**) in a 1,4-fashion. The mid-sized metallabenzene complex **5C** reacts 1,2 with CO_2 , will not react with acetone, and reacts 1,4 with CS_2 .

Another key factor is the geometry of the addition products. In the 1,2-addition products, a strained four-membered ring is formed. This is apparent from the Y–Ir– P_{apical} ($\text{Y} =$ the ring C, O or S) angles of approximately 67° – 71° in the 1,2-products and 86 – 90° in the 1,4-products. This deviation from the ideal 90° in the 1,2-products introduces significant strain in the system and raises the energy of the addition products. This ring strain, however, is mitigated by the conjugated $\text{C}=\text{C}$ bonds that are present in the 1,2- but not the 1,4-addition products. While, in the three acetone additions, the 1,4-addition products (**8Ca**, **8Oa**, and **8Sa**) are lower in energy than the 1,2-addition products (**7Ca**, **7Oa**, and **7Sa**), in the additions of CO_2 and CS_2 , the latter are lower or similar in energy to the former.

Rh Complexes. The cycloaddition reactions were examined with the analogous rhodium complexes (**5***). To the best of our knowledge, there are no reported rhodiaaromatic complexes.^{8,41,96} The results are summarized in Table 4. The calculated cycloaddition reactivities for iridium and for rhodium are nearly identical suggesting that the reaction outcome is metal independent. This is in line with the studies of Thorn and Hoffmann that suggest that rhodium metallabenzene complexes may be stable⁴³ but their formation might be problematic for kinetic reasons.^{41,96}

Summary and Conclusions

We reported here on our DFT investigation at the PCM/mPW1K/SDB-cc-pVDZ//mPW1K/SDD level of theory into the 1,2- and 1,4-cycloaddition reactions of acetone (**a**), CO_2 (**o**), and CS_2 (**s**) to metallabenzene, metallapyrylium, and metallathiabenzene complexes of Ir (**5COS**) and Rh (**5COS***). From the calculated barrier heights and reaction energies, one can note that the calculated reactivities are fully consistent with reported

(95) Woodward, R. B.; Hoffmann, R. *Angew. Chem., Int. Ed. Engl.* **1969**, *8*, 781.

(96) Bleeke, J. R.; Donnay, E.; Rath, N. P. *Organometallics* **2002**, *21*, 4099.

experimental observations.^{31,33,35} For the first time, the complicated reaction patterns of this class of metalloaromatic complexes have been mapped out in detail. Moreover, several factors affecting the reactivity and product distribution were identified. It was found that the metallabenzene complex (**5C**) reacts via a concerted reaction mechanism while the other two (**5O** and **5S**) react in a stepwise manner. The presence of a heteroatom (O or S) in the ring allows for an additional resonance structure whereby an additional ligand can coordinate permitting a stepwise reaction mechanism. The size of the ring and the length of the substrate C=X bond have a significant impact on the reaction barriers. The geometry of the product, including both ring strain and double bond conjugation, also has a dramatic impact. The symmetry of the frontier molecular orbitals, as with most reactions, is also a major factor with 1,2-addition being symmetry forbidden and 1,4-addition symmetry being allowed.

Acknowledgment. Work at the Weizmann Institute of Science was supported by the Helen and Martin Kimmel Center for Molecular Design, the Minerva Foundation (Munich, Germany), and by a grant from Sir Harry Djanogly, CBE. J.M.L.M. is a member of the Lise Meitner-Minerva Center for Computational Quantum Chemistry. M.E.vdB. is the incumbent of the Dewey David Stone and Harry Levine Career Development Chair. M.A.I. acknowledges a Ph.D. fellowship from the Feinberg Graduate School of the Weizmann Institute of Science.

Supporting Information Available: Full coordinates in .xyz format of all complexes are available free of charge at the Unifrom Resource Locator (URL) <http://theochem.weizmann.ac.il/web/papers/cycloaddition.html>. This material is available free of charge via the Internet at <http://pubs.acs.org>.

JA036723A